

## Supplementary Materials and methods

### NKG2D genotyping.

Determination of NKG2D SNP allelic variants was performed using Sequence Specific Primer-Polymerase Chain Reaction (SSP-PCR) as previously described (51). Briefly, genomic DNA was extracted from PBMC from the indicated donors by a modified salting-out method. SSP-PCR was performed with 50 ng of genomic DNA in a total reaction volume of 13  $\mu$ l, using specific primers listed below (0.75–1.5  $\mu$ mol/l) and control primers (0.3  $\mu$ mol/l) (Invitrogen, Paisley, UK). PCR products were visualized in 1.5% agarose gel prestained with ethidium bromide (10 mg/ml). All samples were tested on two separate occasions, and only concurring results were used. SNP alleles were determined on the basis of the presence of a respective PCR product.

1257 G/T	Forward:	5' GCAAAGGAACTTAAGGGCAATAAAAG 3' 5' GCAAAGGAACTTAAGGGCAATAAAAT 3'
	Reverse:	5' TGATTCTCACAAGTGCAAAATATTCCC 3'
1321 G/A	Forward:	5' GTAGAATTAAACCTTCAAAATGCTTCTTCG 3' 5' GTAGAATTAAACCTTCAAAATGCTTCTTCA 3'
	Reverse:	5' AACAAATGCCTGAATAAAATCAGGCTTC 3'
2067 C/G	Forward:	5' CCCAAGATAATATGCTGCTTCTGA 3'
	Reverse:	5' GAGTCATGAAATCAGAATACATCTCTG 3' 5' GAGTCATGAAATCAGAATACATCTCTC 3'
2389 G/A	Forward:	5' TATTGGAGTACTGGAGCAGAACAG 3' 5' TATTGGAGTACTGGAGCAGAACAA 3'
	Reverse:	5' TTTCAGTTAATTAAATGCAACAAGAGGGT 3'
2755 G/A	Forward:	5' GATTTTTGTTGGCGGGCTTGTTTTG 3' 5' GATTTTTGTTGGCGGGCTTGTTTTA 3'
	Reverse:	5' CAATGGCCACAATGACGTGCT 3'
17749 A/T	Forward:	5' GTCAGTATGTGTAGCCCAGTACA 3' 5' GTCAGTATGTGTAGCCCAGTACT 3'
	Reverse:	5' TCTTTGGATATGCAGGGGCATC 3'
37981 G/C	Forward:	5' AGAGAAGGCCAGCAGATCAG 3' 5' AGAGAAGGCCAGCAGATCAC 3'
	Reverse:	5' CCCTGACCCCGTTGGGT 3'

**Figure S1**

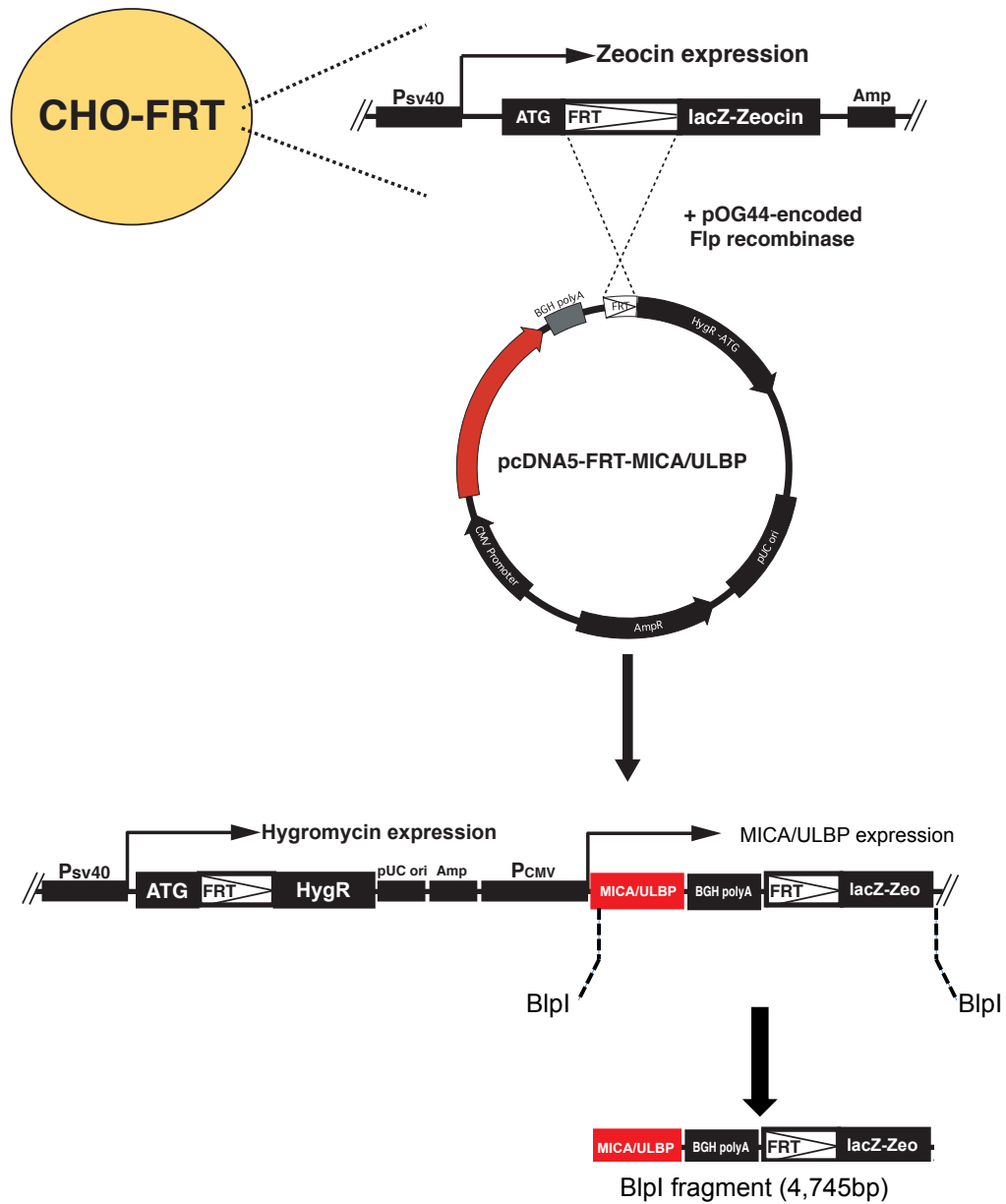


**Figure S1: Schematic representation of the Flp-in system (Invitrogen).**

CHO-FRT cells bearing a unique FRT site were co-transfected with a pOG44 vector encoding Flp recombinase and pcDNA5/FRT containing MICA or ULBP2 cDNAs (shown in red). After integration of the cDNA, cells lose zeocin resistance, but acquire hygromycin resistance. Single integration is then validated by Southern blot: BlnI digestion releases a 4,745bp fragment diagnostic for the linkage of the introduced MICA cDNA to the lacZ-zeo cassette present in the cell line; while the detection of a faint, uniformly-sized band homologous to the small amount of the MICA cDNA probe 5' to the BlnI sites confirms that all integrants are in the same site (see Fig. 1).

## Figure S2

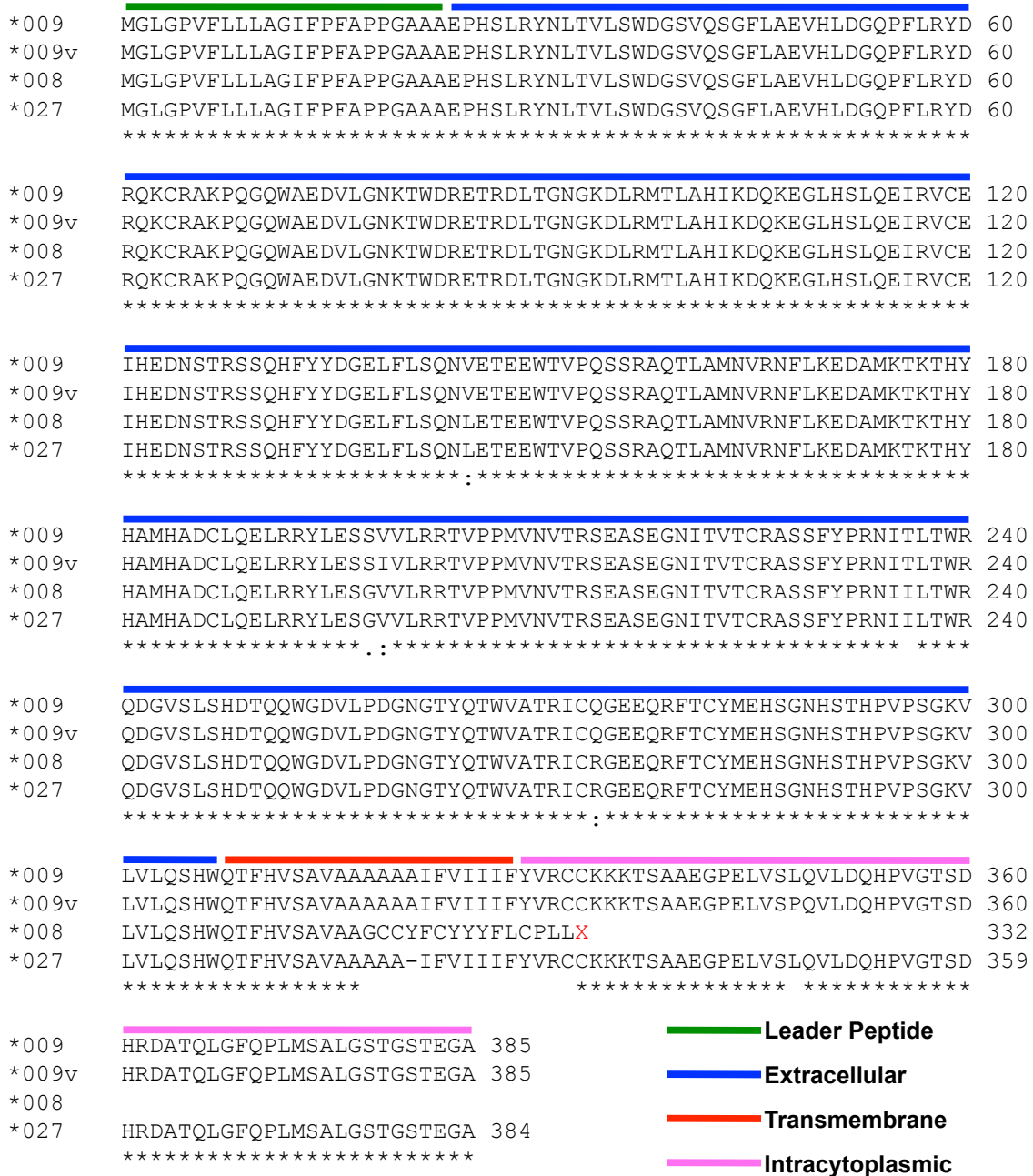


**Figure S2: Alignment of the protein sequences of the MICA alleles used in this study.**

MICA cDNAs were cloned by RT-PCR into the pCR2.1 Topo vector for sequencing before subcloning into pcDNA5/FRT for transfection of CHO-FRT cells. Protein sequences were obtained with the online translation tool from expasy.org and aligned with ClustalW2.0 (S2). Symbol legend: \* identity; : conserved substitution; . semi-conserved substitution; hyphens indicate gaps and the red X in the MICA\*008 sequence indicates the premature stop codon.

**Figure S3**

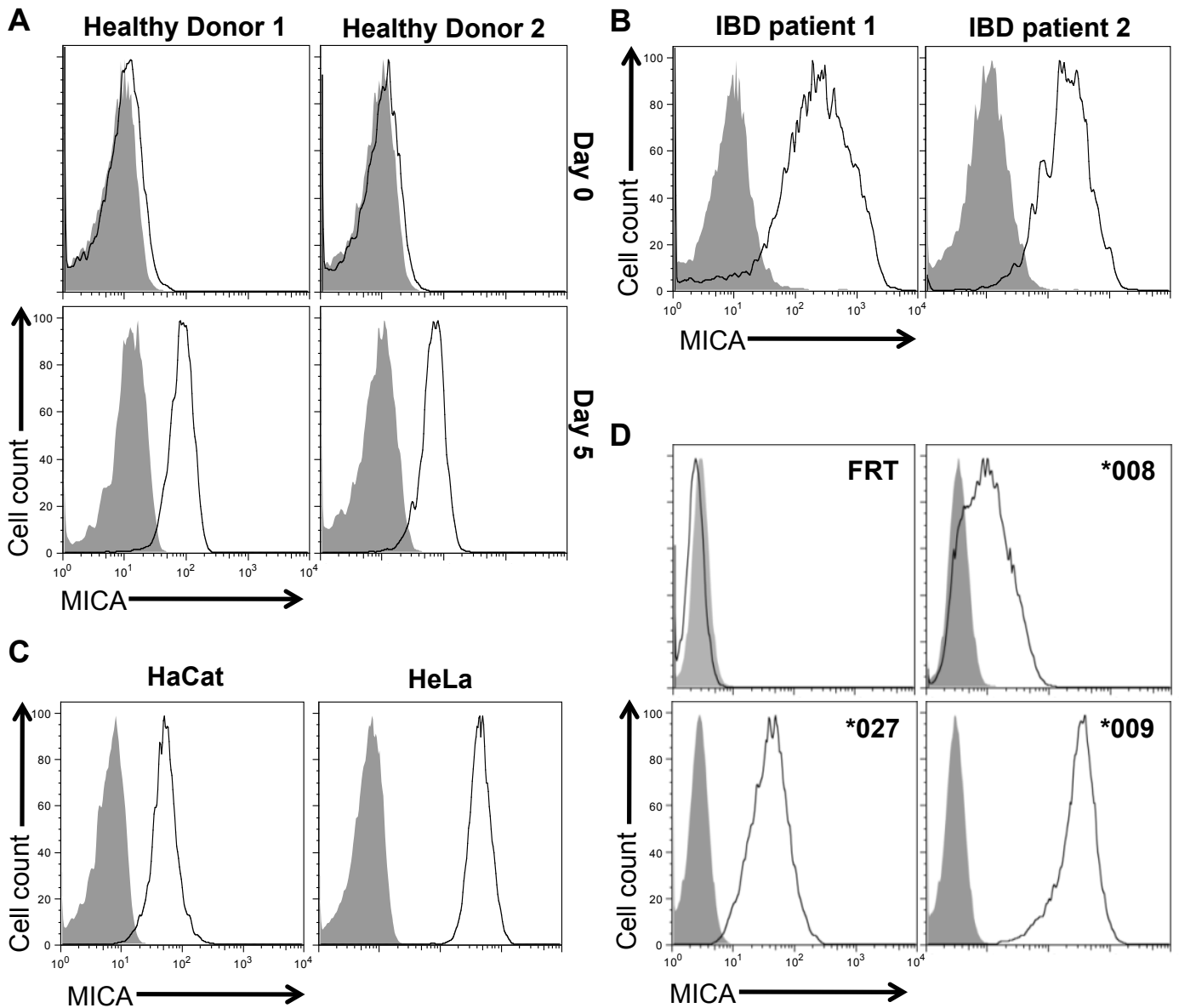


**Figure S3. MICA expression levels in various contexts.**

Flow cytometry analysis on primary samples from different origins or established tumor cell lines, showing a broad range of MICA expression levels: **(A)** on T cells from 2 different donors before (top panels) or 5 days after stimulation with plate-bound anti-CD3 and -CD28 (bottom panels) (MICA MFI:  $10^1$ - $10^2$ ); **(B)** on gut epithelial cells from two donors suspected of presenting inflammatory bowel disease (MICA MFI:  $10^2$ - $10^3$ ); **(C)** on HaCaT (immortalized human keratinocyte cell line) and HeLa (established cervix adenocarcinoma line) (MICA MFI:  $10^1$ - $10^3$ ); **(D)** the range of MICA allelic gene products expressed from CHO-FRT transfectants used in this study (from Fig. 1) (MICA MFI:  $10^1$ - $10^3$ ).

Shaded histogram: Isotype control; open histogram: A647 anti-MICA.

**Figure S4**

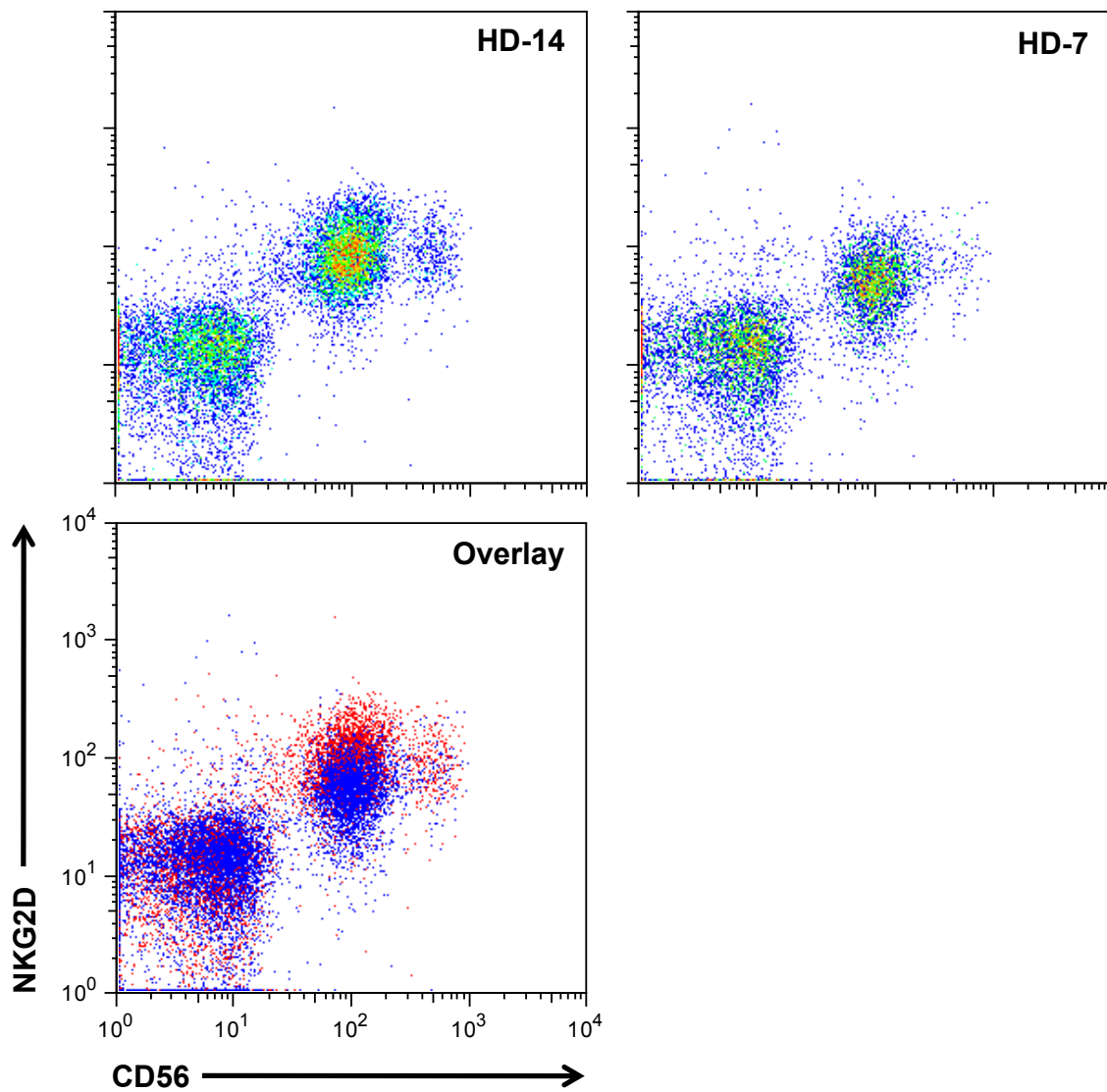


**Figure S4: Representative NKG2D staining on NK cells from 2 donors.**

PBMC were stained with PE-anti-CD3, FITC-anti-CD56 and APC-anti-NKG2D. Top panels show NKG2D staining on NK cells (CD56<sup>(+)</sup>) after gating on CD3<sup>(-)</sup> cells from two donors with the highest (left) and lowest (right) NKG2D MFI (see Table S1). Bottom left panel is the overlay of stainings from the top panels, showing little difference in NKG2D MFI (red, HD-14; blue, HD-7).

**Figure S5**

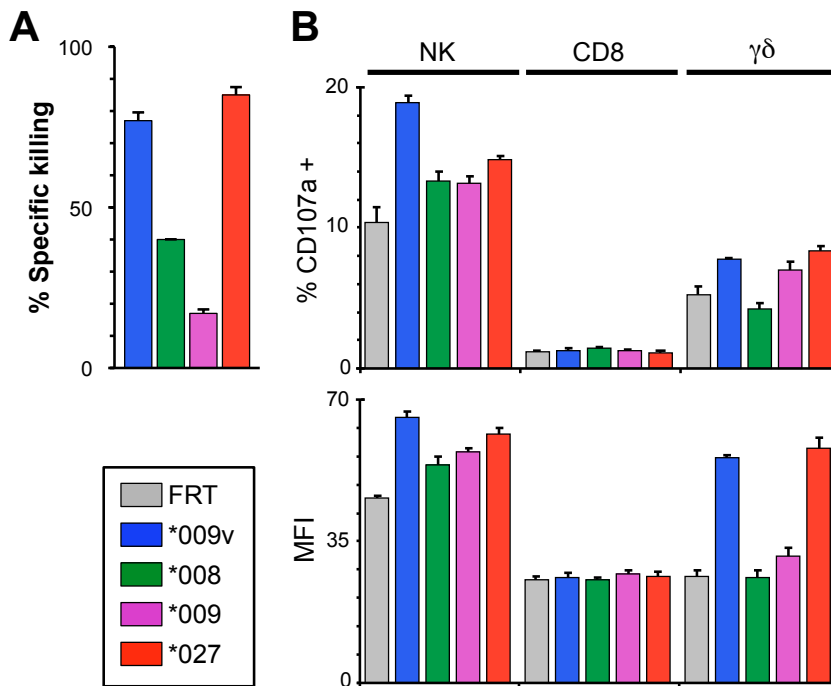


**Figure S5: Killing of CHO-MICA cells and respective activation of NKG2D<sup>+</sup> subsets from an additional donor.**

(A) CFSE assay data as in Fig. 4A. (B) Percentage (top panel) and MFI (bottom panel) of CD107a<sup>(+)</sup> cells in each indicated subset for an additional donor, as described in Fig. 3A and 3B. Data are means of triplicate wells +/- SD.

**Figure S6**

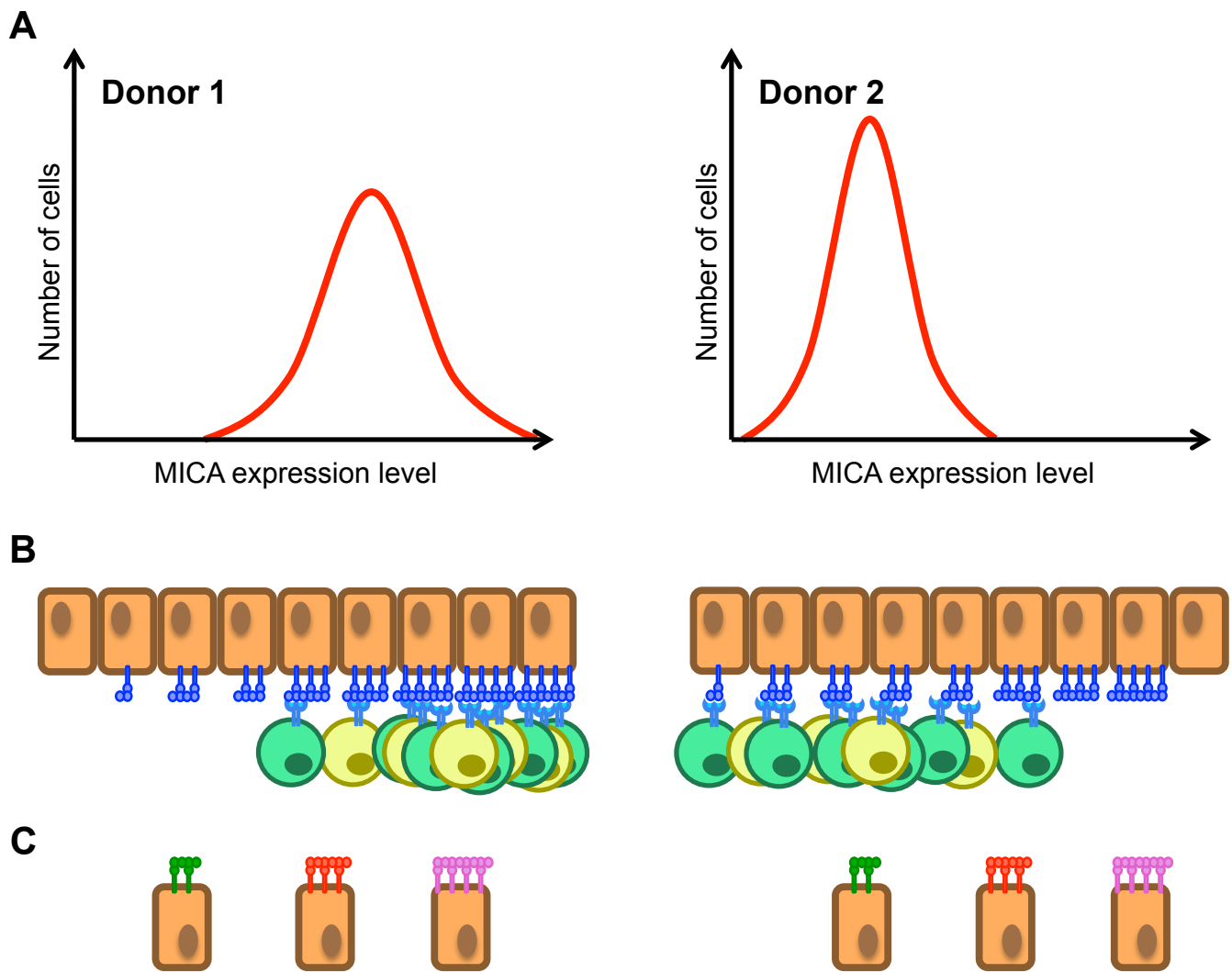


**Figure S6: A schematic of tuning.**

(A) Following dysregulation, MICA levels (red curves, shown on an arbitrary scale) on cells increase to different extents in donors 1 and 2, dictated by their MICA haplotype and other factors. (B) The MICA-responsive  $\gamma\delta$  T (yellow) and NK cells (green) in each donor are activated by the levels of MICA most commonly induced by cellular dysregulation. (C) Defined levels of MICA induction are phenocopied by CHO-FRT cells transfected with specific MICA alleles. Hence targeting of those transfectants depends on the alignment with an individual's MICA-responsive  $\gamma\delta$  T and NK cells.

**Table S1**

		SNPs						Haplotype	Compared to (S3)	
		rs1841958	rs1841957	rs2617171	rs2617170	rs2734565	rs2617160			rs1049174
		1257 G/T	1321 G/A	2067 C/G	2389 G/A	2755 G/A	17749 A/T			37981 G/C
Donor	HD-4	HET	HET	HET	HET	HET	HET	HET	D1/D2	LNK1 / HNK1
	HD-6	HET	HET	HET	HET	HET	A	G	D1/D4	LNK1 / N.D
	HD-16	HET	HET	HET	HET	HET	HET	HET	D1/D2	LNK1 / HNK1
	HD-3	HET	HET	HET	HET	HET	HET	HET	D1/D2	LNK1 / HNK1
	HD-14	G	G	G	A	A	T	C	D3/D3	HNK1 / HNK1
	HD-18	G	A	C	G	A	A	G	D1/D1	LNK1 / LNK1
	HD-17	G	A	C	G	A	A	G	D1/D1	LNK1 / LNK1
	HD-22	G	A	C	G	A	A	G	D1/D1	LNK1 / LNK1

MAIN HAPLOTYPES							
D1	G	A	C	G	A	A	G
D2	T	G	G	A	G	T	C
D3	G	G	G	A	A	T	C
D4	T	G	G	A	G	A	G

**Table S1: NKG2D genotyping from 8 donors used in this study.**

NKG2D SNP allelic variants were identified by SSP-PCR performed on genomic DNA extracted from PBMCs for the indicated donors used in this study as described in Supplementary Materials and Methods. These SNPs were chosen from a panel published in the Ensembl database. Numbering based on the full-length gene is used to describe the position of each base in the NKG2D gene.

HET: Heterozygotes donors; N.D: Not Described in the referenced article.



**Table S2**

	% $\gamma\delta$ TCR <sup>+</sup>	% CD3 <sup>-</sup> CD56 <sup>+</sup>
<b>HD-1</b>	1.6 (96.9%, 88)	11.8 (93%, 64)
<b>HD-2</b>	5.8 (87.9%, 94)	4.9 (96.6%, 88)
<b>HD-3</b>	11.1 (97%, 89)	19 (91.1%, 62)
<b>HD-4</b>	3.4 (92.7%, 85)	10.2 (80.8%, 69)
<b>HD-5</b>	1.1 (90.6%, 90)	4.7 (81.5%, 71)
<b>HD-6</b>	0.8 (85.2%, 87)	10.9 (65.5%, 62)
<b>HD-7</b>	0.8 (79.4%, 79)	8.2 (56.4%, 59)
<b>HD-8</b>	2.4 (88.6%, 92)	9.1 (55.3%, 63)
<b>HD-14</b>	1.7 (94.5%, 153)	33.2 (94.8%, 89)
<b>HD-16</b>	1.1 (87.4%, 97)	15 (82.1%, 72)
<b>HD-17</b>	14.2 (95.3%, 97)	17.7 (85.8%, 78)
<b>HD-18</b>	3.1 (88.6%, 85)	10.4 (74.8%, 63)
<b>HD-22</b>	3.9 (88.5%, 101)	15.1 (73.2%, 67)

**Table S2: Phenotyping of NKG2D<sup>(+)</sup>  $\gamma\delta$  T and NK cells in PBMC from healthy donors.**

PBMC from donors analyzed in Fig. 3 were stained with PE-anti-CD3, FITC-anti-pan  $\gamma\delta$ TCR and APC-anti-NKG2D, or else PE-anti-CD3, FITC-anti-CD56 and APC-anti-NKG2D to determine percentages of circulating NKG2D<sup>(+)</sup>  $\gamma\delta$  T cells and NKG2D<sup>(+)</sup> NK cells. Numbers in parentheses are percentages of NKG2D<sup>(+)</sup> cells within each subpopulation and the mean fluorescence intensity (MFI) for NKG2D, respectively.

## Supplementary references

- S1. A. Antoun, et al. Single nucleotide polymorphism analysis of the NKG2D ligand cluster on the long arm of chromosome 6: Extensive polymorphisms and evidence of diversity between human populations. *Hum. Immunol.* **71 (6)**, 610-620 (2010).
- S2. R. Chenna, et al. Multiple sequence alignment with the Clustal series of programs. *Nucleic Acids Res.* **31**, 3497-3500 (2003).
- S3. T. Hayashi, et al. Identification of the NKG2D haplotypes associated with natural cytotoxic activity of peripheral blood lymphocytes and cancer immunosurveillance. *Cancer Res.* **66 (1)**, 563-570 (2006).